Available online at www.sciencedirect.com
ScienceDirect
Journal of Power Sources 160 (2006) 704–710
JOURNAL OF POWER SOURCES
www.elsevier.com/locate/jpowsour

Evaluation of nano-crystal sized α-nickel hydroxide as an electrode material for alkaline rechargeable cells

Wei-Kang Hu [a,*], Xue-Ping Gao [b], Dag Noréus [c], Trygve Burchardt [a], Nils K. Nakstad [a]

[a] *Revolt Technology AS, Innherredsveien 7, 7014 Trondheim, Norway*
[b] *Institute of New Energy Material Chemistry, Nankai University, Tianjin 300071, China*
[c] *Department of Structural Chemistry, Arrhenius Laboratory, Stockholm University, S-106 91 Stockholm, Sweden*

Received 22 November 2005; received in revised form 6 January 2006; accepted 13 January 2006
Available online 28 February 2006

Abstract

A new synthetic route including a hydrothermal treatment to produce Al-stabilized α-phase nickel hydroxide with an extremely fine grain size but with good crystallinity has been evaluated. The particle size and morphology were characterized by transmission electron microscopy (TEM). The results showed that α-phase nickel hydroxide with nano-sized, well-crystallized particles exhibits not only a high electrochemical capacity of up to 380–400 mAh g^{-1}, but also an excellent rate-capacity performance and long time stability during electrochemical cycling with up to 100% overcharge as well as under a long-term float charge. In contrast, the β-phase nickel hydroxide showed a lower specific capacity and poorer cycling stability under similar overcharge cycling. Except for a lower volumetric energy density than the β-phase, other properties make the Al-stabilized α-phase nickel hydroxide a superior battery material. There is still, however, room to increase the volumetric energy density of the α-phase beyond what is possible to reach by the β-phase via further improvement of the tap density and the specific capacity of the α-phase.

Keywords: Nickel hydroxide; Nanometer sized material; Rechargeable battery; Nickel electrode

1. Introduction

Nickel hydroxide is an importantly functional material with various applications in advanced nickel batteries [1,2], catalysts [3], electrochromic devices [4], electrolysers [5] and ionic exchangers [6]. It exists in two polymorphs known as α- and β-phase. The β-phase nickel hydroxide is widely used as positive materials in the current Ni-based alkaline rechargeable batteries due to a high volumetric electrochemical capacity. This volumetric capacity has also been significantly improved upon by the development of spherical $Ni(OH)_2$ grades with high tap densities. However, the long time stability and reversibility in an alkaline electrolyte is still a cause of concern, especially in sealed cells where the swelling of the nickel electrode after repeated overcharge dries out the already very limited amount of electrolyte. The dry out of the separator caused by the intercalation of water molecules into the nickel electrode is the main cause of degrading cell performance in both NiCd and NiMH batteries. In recent years, a stable α-phase nickel hydroxide as an active material of positive electrodes has attracted much attention [7–24] since it has not only a higher electrochemical capacity per weight, but also a negligible change of electrode volume when charge–discharge cycling between the α- and γ-phase. The small volume change is connected to a low absorption of water molecules during cycling that facilitates cell design and improves the cycling stability. The disadvantage is, however, a lower volumetric energy density compared with the β-phase nickel hydroxide. The theoretical bulk density is 2.82 g cm^{-3} for the α-phase and 3.97 g cm^{-3} for the β-phase, respectively [25]. The theoretical electrochemical capacity of the β-phase is almost reached in practical batteries, leaving room for only marginal future improvements. For the α- to γ-phase conversion, the average oxidation state of nickel in γ-phase nickel oxy-hydroxide was reported to be close to 3.67 [26,27]. This corresponds to an electrochemical capacity of 482 mAh g^{-1}, 66% higher than of that in the β(II)-$Ni(OH)_2$ to β(III)-NiOOH couple (which has a theoretical capacity of 289 mAh g^{-1}). If the theoretical capacity of the α-phase could

* Corresponding author. Tel.: +47 90996625; fax: +47 73533410.
E-mail address: wh@revolttechnology.no (W.-K. Hu).

0378-7753/$ – see front matter © 2006 Elsevier B.V. All rights reserved.
doi:10.1016/j.jpowsour.2006.01.048

be more fully utilized, it would compensate for the lower tap density.

In the present work, we try to improve the specific capacity and long-term stability of the Al-stabilized α-phase nickel hydroxide by synthesizing nano-sized and well-crystallized particles. A stable α-phase nickel hydroxide with a 10 at.% Al substitute was made through optimising chemical precipitation reactions with the assistance of hydrothermal treatments to yield the smallest possible particles having a well-crystallized phase. Herein, we report the synthesis and characterization of this Al-stabilized α-phase nickel hydroxide and its advantages as nickel electrode materials in rechargeable batteries.

2. Experimental

2.1. Preparation and characterization of nano-crystalline α-phase nickel hydroxide

A stable and very fine particle size fraction of Al-stabilized α-phase nickel hydroxide was synthesized by slowly dropping a solution containing $Ni(NO_3)_2{\cdot}6H_2O$ and $Al(NO_3)_3{\cdot}9H_2O$ in a $[Ni^{2+}]/[Al^{3+}]$ ratio of 9:1 into a 0.5N LiOH solution under magnetic stirring at 35 °C. The pH value of the solution after the reaction was in the range of 7.0–7.5. The suspension obtained was kept in the mother solution for 2 h at 35 °C to allow it to settle. Subsequently, it underwent a hydrothermal treatment. The suspension was divided into three parts and sealed in three Teflon autoclaves separately. The three autoclaves were treated at 165 °C for 50, 100 and 150 h, respectively. Afterwards, the autoclaves were cooled down to room temperatures. The blue precipitates obtained were washed with distilled water, filtered and dried at 65 °C. All samples were analyzed by powder X-ray diffraction (XRD) using Cu $K_{\alpha1}$ ($\lambda = 1.5406$ Å) radiation to identify the precipitated phases. Silicon was added as internal standard. The microscopic studies were performed with a FEI Tecnai 20 transmission electron microscopy (TEM).

2.2. Preparation and properties of nickel electrodes

α-Type nickel hydroxide electrodes were prepared by mixing the Al-stabilized α-phase nickel hydroxide (65.6 wt.%) with Ni powder (Inco 210) (26.7 wt.%), cobalt oxide powder (7.7 wt.%) and carboxymethyl cellulose (CMC) as a binder on a nickel foam substrate with a geometrical size of 2.0 cm × 2.0 cm. In order to prevent dropping of active materials from electrodes, two pieces of Ni foam substrates were pressed around the electrode using a pressure of 700–800 kg cm^{-2}. The electrode properties were measured in a half-cell with a 6.0 M KOH solution at 22 °C. An AB_5-type metal hydride (MH) electrode with a capacity in excess of the nickel hydroxide electrode was used as a counter-electrode. A Hg/HgO (6.0 M KOH) electrode was used as reference. The nickel hydroxide electrode was charged at a rate of 0.2 C for 6 h and discharged at a 0.2 C rate to a cut-off potential of 0.1 V. To examine the influence of overcharge on the structure and performances of the α-phase nickel hydroxide, two cycling models with 20% and 100% overcharge and long-term float charge were investigated. The cycling tests were done at a charging rate of 1.0 C and discharging at the same rate to an end potential of 0.1 V. All potential mentioned in this section are with respect to the reference electrode. After repeatedly electrochemical cycles and long-term float charge, the electrodes were removed from the test systems, rinsed with distilled water and dried, after which the active materials were analyzed by XRD.

3. Results and discussion

3.1. Structure and surface morphology

Fig. 1 presents XRD patterns of the four α-phase nickel hydroxide samples prepared in this project as described in Section 2. Samples 2–4 were subject to a hydrothermal treatment at 165 °C for 50, 100 and 150 h, respectively, in order to improve crystallinity. All diffraction peaks of the samples 1, 2 and 3 can be indexed as α-phase nickel hydroxide with a rhombohedral *P*3 structure. In the case of sample 4, however, an extra weak diffraction peak at $2\theta = 19.16°$ was observed though its intensity is weak. The peak was attributed to the (0 0 1) plane of β-phase nickel hydroxide. This implies that a small amount of β-phase nickel hydroxide could be formed after a prolonged hydrothermal treatment.

For the untreated sample 1, the broad diffraction peaks for the (0 0 3) and (0 0 6) planes indicate that the α-phase nickel hydroxide has poor crystallinity. The diffraction peaks of samples 2–4 became sharp, indicating that the sample crystallinity was improved after the hydrothermal treatments. The grain sizes and morphology of the α-phase nickel hydroxide samples were characterized by TEM. Fig. 2 shows the TEM micrographs of the samples 1–3, along with the selected-area electron diffraction (SAED) patterns. As seen in Fig. 2a, the as-prepared sample 1 shows no regular grain morphology. The presence of diffuse rings in the SAED pattern (see Fig. 2b) indicates that the sample has poor crystallinity. The samples 2 and 3 show mixed grain morphology composed of sheet- and rod-like grains (see Fig. 2c and e). The high-resolution TEM image (see Fig. 2g) shows that the rod-like grain has lengths of 50–100 nm and diameters of

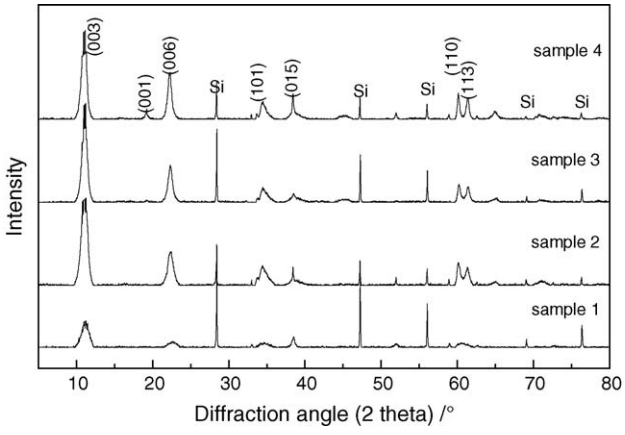

Fig. 1. XRD patterns of the α-phase nickel hydroxide powders using Cu $K_{\alpha1}$ radiation ($\lambda = 1.5406$ Å) with Si internal standard. Sample 1 is as-prepared state. Samples 2–4 have been subjected to a hydrothermal treatment at 165 °C for 50, 100 and 150 h, respectively.

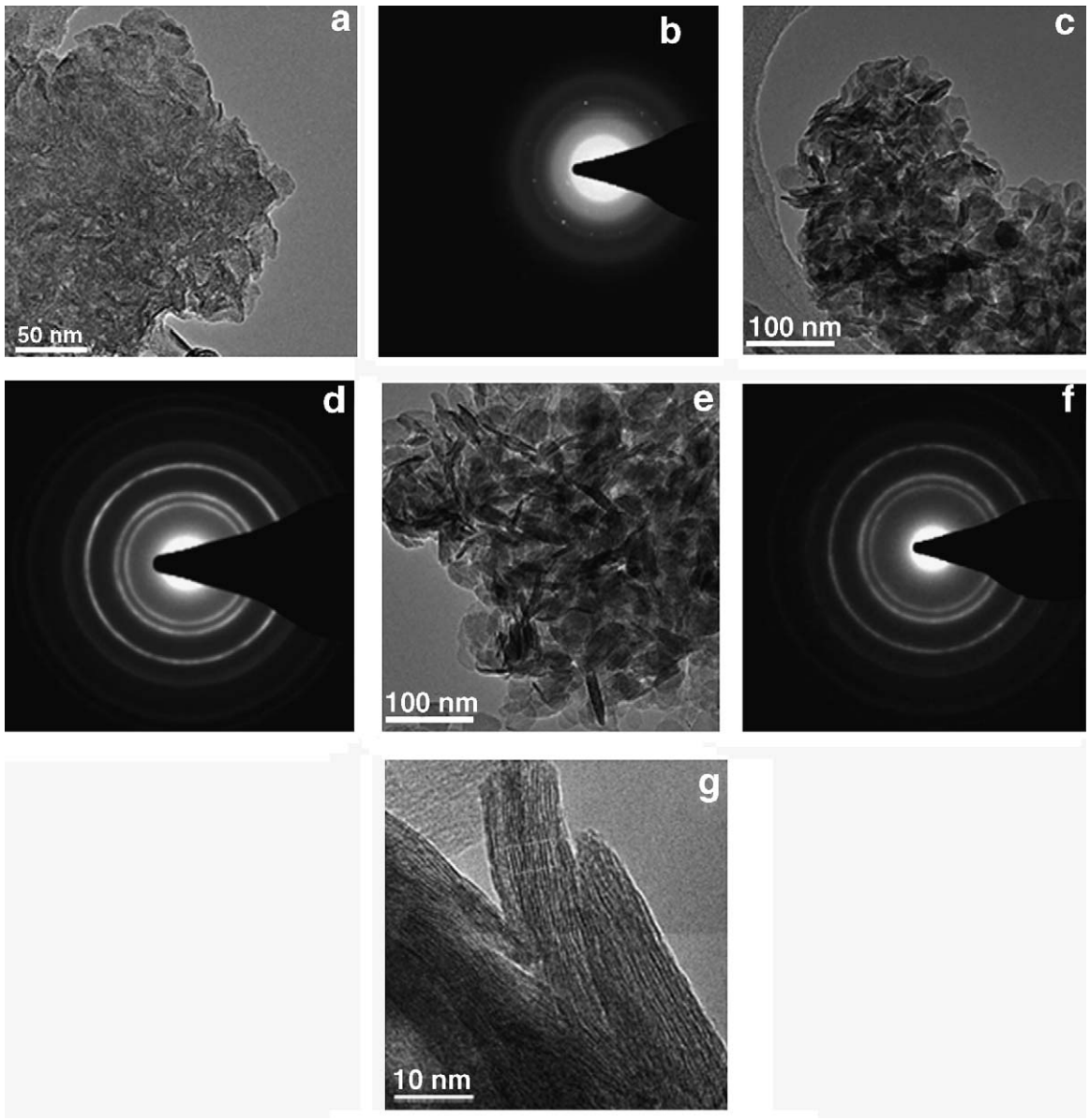

Fig. 2. (a) TEM image of the as-prepared sample 1; (b) electron diffraction pattern of the as-prepared sample 1; (c) TEM image of sample 2; (d) electron diffraction pattern of sample 2; (e) TEM image of sample 3; (f) electron diffraction pattern of sample 3; (g) high-resolution TEM image of sample 3.

approximate 10 nm. The presence of clear poly-diffraction rings in the SAED patterns (see Fig. 2d and f) show that the crystallinity of samples 2 and 3 was considerably improved after the hydrothermal treatments. These results are in good agreement with XRD data. Hydrothermal treatments have also earlier been shown to be very effective in improving the crystallinity of ultra-fine and special shape materials [28–31]. The ultra-fine electrode materials also showed superior physical and chemical properties in the electrochemical energy storage and conversion [32].

3.2. Stability of α-phase nickel hydroxide

The α-phase nickel hydroxide has usually poor stability in a strong basic medium and transforms readily to the β-phase after a few electrochemical charge–discharge cycles [33–36]. However, stability of α-phase nickel hydroxide can be achieved after a 20 at.% substitution of nickel by other metal ions [7–9,12,13,15,24,37–40], in particular with trivalent ions such as Al^{3+} [10,17–19]. But, substitution in the α-phase nickel hydroxide should be as low as possible in order to retain a high capacity and energy density. Hence, a stable α-phase nickel hydroxide having a Al content of only 10 at.% was investigated in this study. In order to probe the stability of the α-phase sample, one part of sample (∼140 mg) was immersed in a 6 M KOH aqueous solution (∼12 mL) for more than 2 months at room temperature with interval stirring. The other part of sample was used as electrode materials for repeatedly electrochemical charge–discharge cycling. Fig. 3 shows the XRD pattern of the α-phase sample after being left in the 6 M KOH for 65 days. As can be seen, the product still retains the α-phase structure and no β-phase diffraction peak was detected in the pattern. After repeatedly

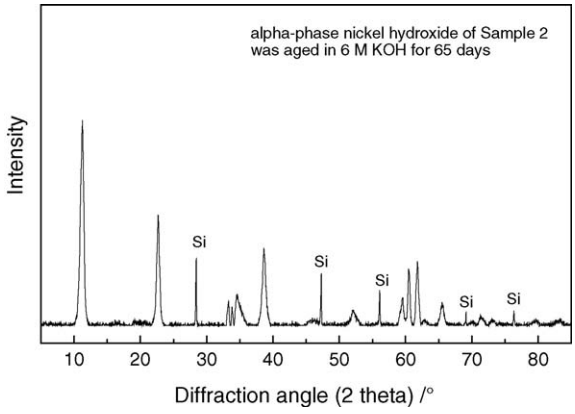

Fig. 3. XRD pattern of the α-phase nickel hydroxide (sample 2) using Cu $K_{\alpha 1}$ radiation (λ = 1.5406 Å) with Si internal standard. The sample was left in 6 M KOH for 65 days at room temperature.

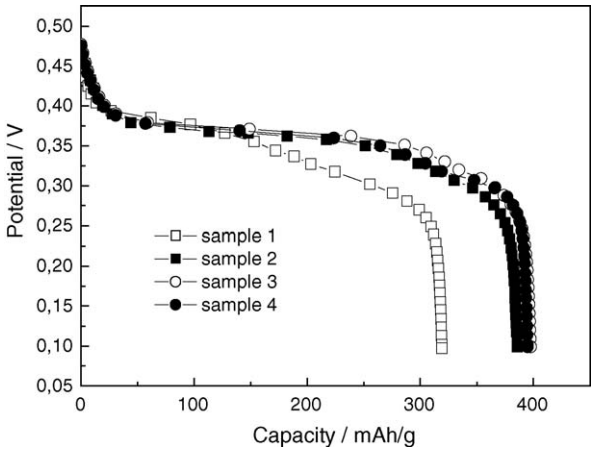

Fig. 5. Discharge curves of the four α-phase nickel hydroxide electrodes at a rate of 0.2 C. Sample 1 is as-prepared state. Samples 2–4 have been subjected to a hydrothermal treatment at 165 °C for 50, 100 and 150 h, respectively.

electrochemical charge–discharging for 500 cycles, the electrode material still keeps the α-phase (as shown in Fig. 9). These results indicate that the Al-substituted α-phase nickel hydroxide with only 10 at.% Al has enough stability in strong basic medium to be used as electrode materials.

The thermogravimetric (TG) analyses of the α- and β-phase nickel hydroxide with a heating rate of 2.0 °C min^{-1} in Ar atmosphere are shown in Fig. 4. The results show that the α-phase sample loses weight in two steps. The first stage with a weight loss of ∼10% (room temperature to 100 °C) is due to the loss of intercalated species in the interlayer region. The intercalated species are mainly the water molecules and small amounts of anions (NO_3^- in this study). The second weight loss at temperature of ∼250 °C is ascribed to the decomposition of the nickel hydroxide into oxide. By comparison, the β-phase sample exhibits only one weight loss step (∼250 °C) corresponding to the decomposition reaction of $Ni(OH)_2 = NiO + H_2O$. The experimental weight loss is ∼17.5%, close to the theoretical value of 18%. The TG measurements show that the α-phase nickel hydroxide has more adsorbed/intercalated water

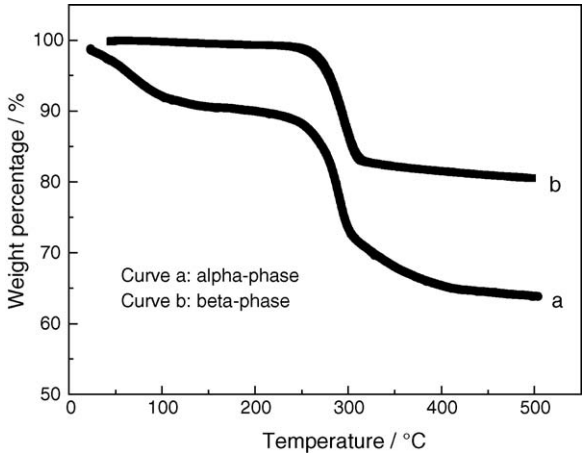

Fig. 4. TG curves of: (a) α-phase nickel hydroxide (sample 3) and (b) commercial β-phase nickel hydroxide with a heating rate of 2 °C min^{-1} in Ar.

molecules. The larger interlayer spacing in the α-phase with the *c* axis of ∼7.9 Å permits intercalation of water molecules and anions, compared with the compact layered β-phase structure with a c parameter of 4.6 Å that does not allow intercalation of any specie in its interlayer region [41]. The intercalated water in the α-phase nickel hydroxide may play an important role to improve the rate-capacity performance of electrodes, as described in the following section.

3.3. Electrode properties

Fig. 5 shows the discharge curves of the four sample electrodes. As can be seen, the sample 1 had the electrochemical capacity of 320 mAh g^{-1}. The other three samples had capacities in the range of 380–400 mAh g^{-1}. The higher capacity of the samples 2–4 was attributed to their good crystallinity, as indicated in Fig. 1. However, a prolonged hydrothermal treatment did not further increase the electrochemical capacity. Instead the risk of forming the β-phase nickel hydroxide increased, as shown by the appearance of the (0 0 1) β-phase reflection in Fig. 1, for the longest hydrothermal treatment. A well-crystallized single α-phase nickel hydroxide with a higher capacity can thus be obtained using a relatively short treatment period of 50–100 h at 165 °C.

Fig. 6 shows the relationship between the discharge capacity and discharge rates from 0.2 to 20 C at 22 °C. The rate-capacity performance of commercial β-phase nickel hydroxides is also presented for comparison. The α-type nickel hydroxide can sustain very high discharge rates, being able to maintain 67% and 41% of the nominal capacity at the discharge rates of 10 and 20 C, respectively. This is significantly better than the β-type nickel electrodes, as seen in Fig. 6. The superior rate capability of the α-phase nickel hydroxide is probably related to its larger interlayer spacing about 7.9 Å, allowing for a better proton mobility compared with the β-phase nickel hydroxide having an interlayer distance of 4.6 Å.

The proton is intercalated in the nickel oxy-hydroxide during discharge as electrons are consumed by the electrochemical

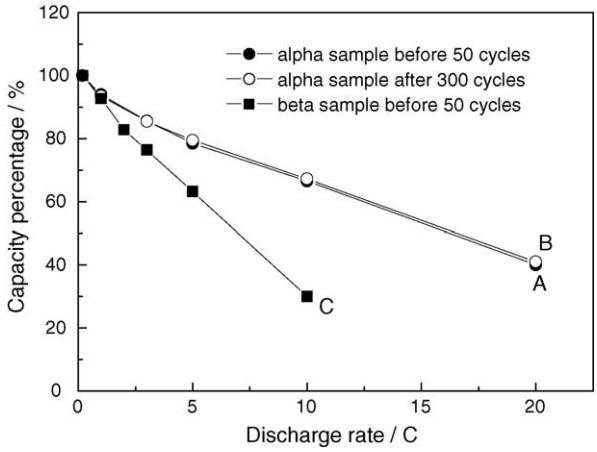

Fig. 6. Available discharge capacity using discharge current from 0.2 to 20 C at 22 °C. Curves A and B are the α-phase nickel hydroxide electrodes (sample 3) before cycling and after 500 cycles, respectively. Curve C is the β-phase nickel hydroxide electrode.

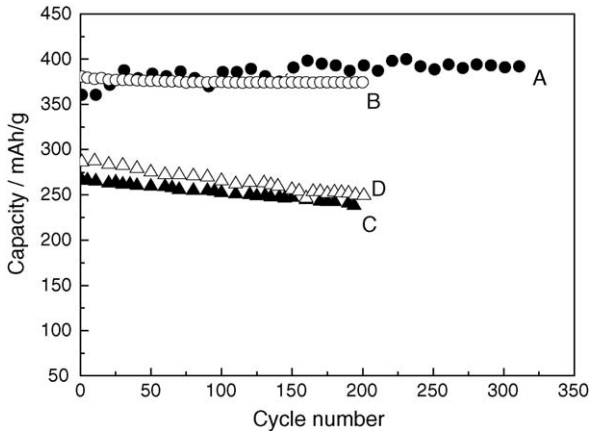

Fig. 7. Discharge capacity vs. cycle number at a charge–discharge rate of 1.0 C. Curves A and B are the α-phase nickel hydroxide electrodes under 20% and 100% overcharge, respectively. Curves C and D are the β-phase nickel hydroxide electrode with 20% and 100% overcharge, respectively.

reaction of $Ni^{n+}OOH + H^+ + (n-2)e^- = Ni(OH)_2$ $(3 < n < 4)$. Water and OH^- play an important role in the proton transport [42]. When the discharge rate increases, a faster proton consumption (intercalation) reaction is needed. With the larger interlayer distance leading to a higher mobility of the intercalated water molecules, the replenishment of protons at the reaction interface is supposed to work faster than in the β-phase nickel hydroxide. It results in a better rate-capacity performance with low polarization in the α-phase nickel hydroxide at high discharge rates. A slightly higher discharge potential in the α-phase nickel hydroxide is also probably related to the larger interlayer distance that facilitates the mass transport during the charge–discharge processes. Other researchers [17] also observed the lower internal resistance of α-phase nickel electrodes compared with the β-phase nickel electrodes.

3.4. Influence of overcharge on cycling stability and structure

The evolution of the discharge capacity as a function of the cycle number using an overcharge of 20% and 100% is shown in Fig. 7. The α-phase samples exhibited good lifespan and stability even after several hundred cycles. The dependence of discharge capacity on the cycle number of β-phase samples is also shown in Fig. 7. As can be seen, the electrochemical capacity of the β-phase nickel hydroxide faded with cycling. This is related to the β-phase nickel hydroxide being partly converted to the γ-phase structure as the electrodes are repeatedly overcharged. Fig. 8 reveals the XRD patterns of the β-phase nickel hydroxide before and after the overcharge cycling. Diffraction peaks from the γ-phase nickel hydroxide was detected after 200 cycles with 100% overcharge. A significant increase of electrode volume and mechanical deformation were also observed concomitantly with the formation of the γ-phase structure. The swelling of electrode volume causes it to crack with a loss of contact between active materials and current collectors [43], leading to the observed capacity loss.

In contrast, under the same overcharge conditions the α-phase nickel hydroxide showed a better stability in the α-/γ-phase conversion. Fig. 9 shows the XRD pattern of the α-phase samples after 300 charge–discharge cycles with 20% overcharge and subsequent 200 charge–discharge cycles with 100% overcharge. The sample still retains the α-phase structure and no β-phase diffraction peak was detected, indicating excellent reversibility in the α-/γ-phase transformation.

Rechargeable alkaline batteries are also good candidates for back-up power. The batteries used in such applications, however, must be able to withstand long-term float charging. Thus, the effect of float charge on the structural stability of the α-phase nickel hydroxide was examined. Fig. 10 shows the XRD pattern of the α-phase nickel hydroxide electrode after undergoing a float charge for 1 month at a rate of 0.2 C. No extra peaks in the diffraction pattern are observed, indicating that the α-phase sample has excellent phase-structural stability when being subject to a long-term float charging.

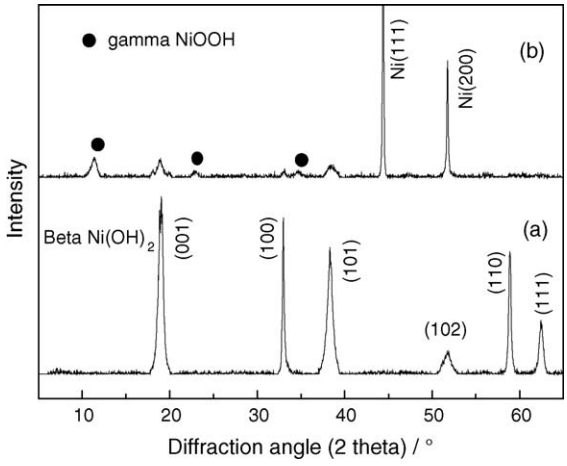

Fig. 8. XRD patterns of the β-phase nickel hydroxide electrodes: (a) before cycling and (b) after 200 cycles at 1.0 C rates with 100% overcharge.

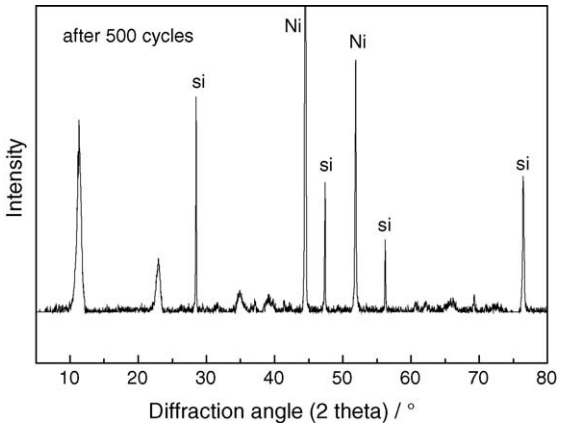

Fig. 9. XRD patterns of the α-phase nickel hydroxide (sample 3) after 300 cycles with 20% overcharge and subsequent 200 cycles with 100% overcharge at 1.0 C rates.

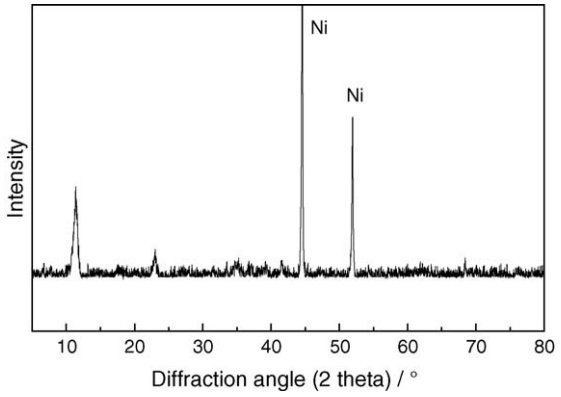

Fig. 10. XRD pattern of the α-phase nickel hydroxide (sample 3) after float charge at 0.2 C and 22 °C for 1 month.

4. Conclusions

The better stability of the α-phase nickel hydroxide over the β-phase nickel hydroxide makes it a promising candidate as battery materials in the rechargeable alkaline Ni-based batteries and Ni–H_2 batteries. The main and important advantages of the α- to γ-nickel hydroxide phase transformation compared to the β-phase are thus a higher specific capacity, due to the higher number of exchanged electrons, about 1.38 per nickel atom in this case. It has also better rate-capacity performance and better repeating cycle stability, especially under long-term overcharge cycling and float charge. The disadvantage of the α-phase nickel hydroxide is its lower tap density due to a large interlayer spacing, leading to the lower volumetric energy densities. In this work, the tap density of the α-phase nickel hydroxide is about 1.2 g cm^{-3}, which is less than half of the theoretical bulk density of 2.83 g cm^{-3}. Therefore, it is still possible to improve the tap density by for example developing a spherical high-density α-phase nickel hydroxide, similar to what was done for the β-phase nickel hydroxide several years ago [44]. In addition, there is also some room for increasing the specific capacity from the present 380 towards the theoretical value of 482 mAh g^{-1}. The β-phase nickel hydroxide for current battery use has a tap density of 2.1–2.2 g cm^{-3} and a practical capacity is close to the theoretical limit at 289 mAh g^{-1}. This gives a volumetric capacity of 620–640 mAh cm^{-3}. The α-phase nickel hydroxide reported here reached about 75% of this. With only a modest improvement of the tap density and specific capacity, it is clear that the α-phase nickel hydroxide will have high potential applications in the future rechargeable alkaline NiFe, NiZn, NiCd, NiMH and Ni–H_2 batteries.

The nano-sized and well-crystallized α-phase nickel hydroxides used in this work were synthesised by a chemical co-precipitation with a subsequent hydrothermal process. TEM observations show that the α-phase nickel hydroxide particles have mixed grain morphology of sheet- and rod-like shapes after the hydrothermal treatments. XRD and SAED examinations verified that the crystallinity of the α-phase structure was improved by a hydrothermal treatment for 50–100 h at 165 °C. The hydrothermal treated samples reached a higher electrochemical capacity of up to 380–400 mAh g^{-1}, about 30% higher than the theoretical capacity of current β-phase nickel electrodes.

Acknowledgement

This work was partly supported by the 973 Program (2002CB211800) of China.

References

[1] J. McBreen, in: R.E. White, J.O.M. Bockris, B.E. Conway (Eds.), Modern Aspects of Electrochemistry, vol. 21, Plenum Press, New York, 1990, p. 29.
[2] (a) P. Oliva, J. Leonardi, J.F. Laurent, E. Demas, J.J. Braconis, M. Figlanz, F. Fievet, A. Deguibert, J. Power Sources 8 (1982) 229;
(b) Z.S. Wronski, Int. Mater. Rev. 46 (2001) 1.
[3] (a) A. Andreev, P. Khristov, A. Losev, Appl. Catal. B 7 (1996) 225;
(b) K.M. Lee, W.Y. Lee, Catal. Lett. 83 (2002) 65–70;
(c) Y. Yuan, K. Asakura, H.L. Wan, K. Tsai, Y. Iwasawa, Chem. Lett. 9 (1996) 755.
[4] (a) K.S. Ahn, Y.C. Nah, Y.E. Sung, K.Y. Cho, S.S. Shin, J.K. Park, Appl. Phys. Lett. 81 (2002) 3930;
(b) S.I. Cordoba-Torresi, C. Gabrielli, A. Hugot-Le Goff, R. Torresi, J. Electrochem. Soc. 138 (1991) 1548.
[5] D.E. Hall, J. Electrochem. Soc. 130 (1983) 317.
[6] N. Mikami, M. Sasaki, S. Horibe, T. Yasunaga, J. Phys. Chem. 88 (1984) 1716.
[7] L. Demourgues-Guerlou, C. Delmas, J. Electrochem. Soc. 143 (1996) 561.
[8] L. Demourgues-Guerlou, J.J. Braconnier, C. Delmas, J. Solid State Chem. 104 (1993) 359.
[9] C. Faure, C. Delmas, P. Willmann, J. Power Sources 36 (1991) 497.
[10] K.T. Ehlsissen, A. Delahaye-Vidal, P. Genin, M. Figlarz, P. Willmann, J. Mater. Chem. 3 (1993) 883.
[11] C.Y. Wang, S. Zhong, D.H. Bradhurst, H.K. Liu, S.X. Dou, J. Alloys Compd. 802 (2002) 330–332.
[12] P.V. Kamath, M. Dixit, L. Indira, A.K. Shukla, V.G. Kumar, N. Munichandraiah, J. Electrochem. Soc. 141 (1994) 2956.
[13] M. Dixit, P.V. Kamath, J. Gopalakrishnan, J. Electrochem. Soc. 146 (1999) 79.
[14] R.S. Jayashree, P.V. Kamath, J. Appl. Electrochem. 31 (2001) 1315.
[15] R.S. Jayashree, P.V. Kamath, J. Power Sources 107 (2002) 120.
[16] V. Ganesh Kumar, N. Munichandraiah, P.V. Kamath, A.K. Shukla, J. Power Sources 56 (1995) 111.
[17] A. Sugimoto, S. Ishida, K. Hanawa, J. Electrochem. Soc. 146 (1999) 1251.
[18] J. Dai, S.F.Y. Li, T.D. Xiao, D.M. Wang, D.E. Reisner, J. Power Sources 89 (2000) 40.
[19] G.A. Caravaggio, C. Detellier, Z. Wronski, J. Mater. Chem. 11 (2001) 912.

[20] (a) H. Chen, J.M. Wang, T. Pan, Y.L. Zhao, J.Q. Zhang, C.N. Cao, J. Electrochem. Soc. 150 (2003) A1399;
(b) J. Bauer, D.H. Buss, H.J. Harms, O. Glemser, J. Electrochem. Soc. 137 (1990) 173.
[21] H. Zhang, H. Liu, X. Cao, S. Li, C. Sun, Mater. Chem. Phys. 79 (2003) 37.
[22] W.K. Hu, D. Noréus, Chem. Mater. 15 (2003) 974.
[23] P. Jeevanandam, Yu. Koltypin, A. Gedanken, Nano Lett. 1 (2001) 263.
[24] B. Liu, X.Y. Wang, H.T. Yuan, Y.S. Zhang, D.Y. Song, Z.X. Zhou, J. Appl. Electrochem. 29 (1999) 855.
[25] M. Oshitani, T. Takayama, K. Takashima, S. Tsuji, J. Appl. Electrochem. 16 (1986) 403.
[26] D.A. Corringan, S.L. Knight, J. Electrochem. Soc. 136 (1989) 613.
[27] Z.Y. Xu, B.C. Cornilsen, G. Meitzner, Proc. Electrochem. Soc. 98–115 (1999) 1–10 (selected battery topics).
[28] E. Matijevi, Chem. Mater. 5 (1993) 412.
[29] K. Matsui, T. Kyotani, A. Tomita, Adv. Mater. 14 (2002) 1216.
[30] X. Wang, Y.D. Li, J. Am. Chem. Soc. 124 (2002) 2880.
[31] Y.P. Fang, A.W. Xu, L.P. You, R.Q. Song, J.C. Yu, H.X. Zhang, Q. Li, H.Q. Liu, Adv. Funct. Mater. 13 (2003) 955.
[32] (a) P. Poizot, S. Laruelle, S. Grugeon, L. Dupont, J.M. Tarascon, Nature (2000) 496;
(b) M. Holzapfel, H. Buqa, W. Scheifele, P. Novak, F.M. Petrat, Chem. Commun. (2005) 1566;
(c) W.K. Hu, X.P. Gao, M.M. Geng, Z.X. Gong, D. Noréus, J. Phys. Chem. B 109 (2005) 5392;
(d) Y.S. Zhang, Z. Zhou, J. Yan, J. Power Sources 75 (1998) 283.
[33] A. Delahaye-Vidal, B. Beaudoin, N. Sac-Epee, K. Tekaia-Elhsissen, A. Audemer, M. Figlarz, Solid State Ionics 84 (1996) 239.
[34] H. Bode, K. Dehmelt, J. Witte, Electrochim. Acta 11 (1966) 1079.
[35] R.S. McEwen, J. Phys. Chem. 12 (1971) 1782.
[36] F. Portemer, A. Delahaye-Vidal, M. Figlarz, J. Electrochem. Soc. 139 (1992) 671.
[37] C. Delmas, J.J. Braconnier, Y. Borthomieu, P. Hagenmuller, Mater. Res. Bull. 22 (1987) 741.
[38] C. Faure, C. Delmas, M. Fouassier, P. Willmann, J. Power Sources 35 (1991) 249.
[39] C. Faure, C. Delmas, M. Fouassier, P. Willmann, J. Power Sources 35 (1991) 263.
[40] L. Demourgues-Guerlou, C. Delmas, J. Power Sources 52 (1994) 275.
[41] R. Barnard, C.F. Randell, F.L. Tye, J. Appl. Electrochem. 10 (1980) 109.
[42] W.J. Moore, Physical Chemistry, 5th ed., 1972, p. P435.
[43] D. Singh, J. Electrochem. Soc. 145 (1998) 116.
[44] M. Oshitani, K. Takashima, Y. Matsumara, Proc. Symp. Nickel Hydroxide Electrodes, 1989, Proc. Electrochem. Soc. 90–94 (1990) 197–214.